Comparison of harmonic emission in LV side of a large grid connected PV power plant

A. Carretero-Hernandez, E. Artigao, S. Martin-Martinez, C. Alvarez-Ortega, M. Ochoa-Gimenez, E. Gomez-Lazaro

***Abstract*—The use of solar photovoltaic (PV) in distribution networks has increased considerably in recent years. Although they have many advantages, PV systems can also result in complex power quality issues in distribution networks, like harmonic distortion, that can interfere with loads and controllers. Harmonic emission from different inverters and their aggregation is thus of interest. In this work, harmonic emission of two PV string inverters and two substations operating in a large PV power plant is presented. The distribution of the full range of current harmonics is analyzed, as well as the correlation between the values of each harmonic and the power level produced, by the inverter or substation, and the correlation between voltage and current harmonics. Significant differences are observed in the harmonic emission of the inverters, despite being under the same operating loading and grid conditions. The results obtained for the substations are in line to those for the inverters. This study was performed in a grid connected 12 MW PV power plant operating in Europe.**

***Keywords*—Electric power system, harmonics, string inverter, PV power plant, substation.**

I. Introduction

RENEWABLE energy is being increasingly used worldwide. In 2021, nearly 257 GW of new renewable energy was added, increasing the stock of renewable power by 9.1% and contributing to 81% of new power additions globally. Over half of those renewable energy additions were made up of solar photovoltaic (PV) power alone, which reached a record 133 GW [1]. The top 3 countries in new solar capacity installation that year were China (54.9 GW), the United States (27.3 GW) and India (14.2 GW). With regard to Europe, Germany, Spain and Poland are among the top 10 global solar markets with 6.0 GW, 4.8 GW and 3.8 GW of new installations that year, respectively [2]. Under this scenario, the utility-scale category accounts for the majority of the installations, although solar PV systems installed at the rooftop level have recently increased in size in distribution networks.

PV systems have a number of benefits, but can also cause complex power quality problems in distribution networks, such as harmonic distortion, which has an inverse linear relation with solar insolation (thus, power loading) increased by the presence of voltage supply disturbances [3]. The negative impacts caused by high PV penetration include reverse power flow, overvoltage along distribution feeders, voltage control difficulty, phase unbalance, increased reactive power, islanding detection difficulty and power quality problems (harmonics) [4]. Therefore, harmonic distortions, which can originate from a number of sources, have emerged as a significant issue [5]. In addition, the growing usage of power electronics-based nonlinear loads and harmonic-inducing penetrations of PV systems into the network cause poor power quality, which, in turn, causes equipment to overheat and control systems to fail [6].

Solar PV generation systems need a power electronic interface to connect to the grid, which is commonly an inverter. Modern inverters should have low harmonic emissions, and must ensure compliance with defined harmonic emission limits defined by different standards. For medium-large PV systems, IEEE standard 519-2022 focuses on the network's permitted harmonic distortion levels. The grid interconnection requirements of the distributed resources are outlined in IEEE standard 1547-2018. Further IEC standards exist for disturbing equipment installations for PV systems (IEC 61000-3-6) in European countries. In other countries, like UK, for instance, EREC G5-5 is applied for different operating voltages, or IEEE 519 in US. In all cases these standards apply to the point of common coupling (PCC) and not to the internal low voltage grid of the PV plants but can be used as a reference for emission levels. However, modern PV inverters may display different power-dependent variations in performance, often characterized by increased harmonic and interharmonic emissions [7], which are not considered in the standards. In this sense, the dependence, or no-dependence, of the power flow on the harmonics influences their emission and aggregation. It is also important to highlight the level of dependence of each harmonic. In this way it is possible to characterize the harmonic distortion in the internal low voltage network of the photovoltaic plant beyond the levels proposed by the standards in the PCC. Therefore, it is crucial to identify the harmonics generated by the grid-connected PV inverter system under various operating scenarios. In this regard, several power quality assessment guidelines can be found in the literature, aimed at mitigating the shortcomings of the above-mentioned standards, such as in [8] and [9].

The harmonic current levels caused by PV inverters employed in distributed generation have been widely studied in the literature but are limited to simulated data and low

This work was fully supported by SBPLY/19/180501/000287 and partially supported by PID2021-126082OB-C21.

A. Carretero-Hernandez, S. Martin-Martinez, E. Artigao, and E. Gomez-Lazaro are with the Department of Electrical Engineering, IIER, Universidad de Castilla-La Mancha, Spain 02071 (e-mail of corresponding author: alejandro.carretero1@alu.uclm.es; e-mails: estefania.artigao@uclm.es, sergio.martin@uclm.es, emilio.gomez@uclm.es).

C. Alvarez-Ortega is with GoodWe, Spain. (e-mail: carlos.alvarez@goodwe.com).

M. Ochoa-Gimenez is with Huawei, Spain.(e-mail: miguel.ochoa@huawei.com).

Paper submitted to the International Conference on Power Systems Transients (IPST2023) in Thessaloniki, Greece, June 12-15, 2023.

power capacities. The authors in [6] and [3] studied the total harmonic distortion (THD) using simulated data of a 1.2 MW PV power system up to harmonic 31. Similarly, the authors in [4] simulated a 4 MW PV system and analyzed up to harmonic 15. More studies using simulated data and studying the THD and harmonics up to 29 were presented in [5], [10], [11]. Harmonic modeling was performed in [12]. Another common approach for the analysis of harmonic and interharmonic distortion is laboratory testing, as described in [13], [14], [15] for different operating conditions. Regarding harmonic emissions of operating PV power plants, a study was performed by [16] on an 800 kWp plant using a Class-A PQ analyzer for the measurement campaign. The outcomes demonstrated that harmonic current emission substantially depends on the level of PV power generation, reaching maximum values at both power output extremes.

In contrast to the above-mentioned studies carried out in small sites and/or using simulated data, this paper presents the analysis of the harmonic emissions of a large PV power plant of over 12 MW in operation in Europe. The present work characterizes, in depth, the harmonic emissions measured at the AC side of two different high power string inverters and at the LV side of two different substations. For this characterization, 3 independent studies were established with a complete analysis of the 50 current harmonics. In the first study, the relative harmonic ranges present both in the inverters and in the low voltage side of the substations were represented. The second study aimed to establish the relationship between the generated power level and the measured harmonics. Finally, the intention of the third study was to establish the relationship between current harmonics and voltage harmonics.

The rest of the work is structured as follows. The database used for the analysis is described in section II, while section III details the methodology used for the analysis. The results are presented in section IV and further discussed in section V. Finally, section VI summarizes the conclusions of the current research.

II. Data base

A measurement campaign was performed in a large grid-connected utility scale PV power plant of over 12 MW operating in Europe. Figure 1 depicts a diagram of the solar farm. It consists of 4 different substations of around 3 MW each, gathering a different number of inverters of two different models and rated powers, as shown. The data were collected using the Fluke TM 1760, which is a Class-A PQ analyzer (from Fluke Corporation, USA), over a period of 5 weeks. The Fluke TPS FLEX 24 Flexible Current Probe were used in the present study. According to the manufacturer, these present 1% intrinsic error and 0.5° phase error, both of measuring range at 23°C ±2 K; 74°F ±2 K, for 48 to 65 Hz. Altogether, the equipment is able to conduct tests according to the stringent international IEC 61000-4-30:2015+A1:2021 Class-A standard. Four measurement points were defined, two in the AC side of two different string inverters (thereafter, inverter A and inverter B), and two more in the low

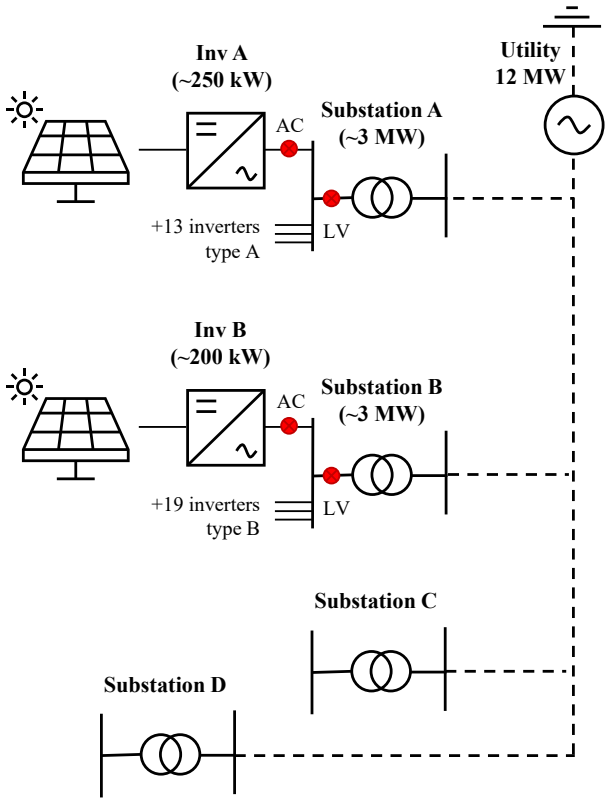

Fig. 1: Utility-scale PV plant layout.

voltage (LV) side of two different substations (hereafter, substation A and substation B), as illustrated in Figure 1, where the red round marks represent the position of the mentioned measurement points. The inverters were chosen so that they had the same distance to their respective substation (inverter A to substation A, and inverter B to substation B). The data include standard-day, and 10-minute and 1-minute mean values for voltage, current, active power, reactive power, power factor and apparent power, with data recorded at 3-second intervals. Voltage and current harmonics were calculated based on a 10/12 cycle (200 ms) averaging interval. This interval contains exactly 2048 sample values. From these samples, 1024 FFT bins (5 Hz) were calculated. The harmonics were then obtained using a gapless harmonic subgroup assessment. The interharmonics were obtained using a gapless interharmonic-centered subgroup assessment. The harmonics and interharmonics calculations follow the IEC 61000-4-7:2002+A1:2009 standard, section 5.6 (no smoothing).

III. Methodology

The aim of the present work was to analyze harmonic emissions at four different points of a large utility-scale PV power plant in operation. To this end, three different comparative studies were performed (shown in section IV), the calculations for which are now described.

For the first study, it was necessary to obtain the distribution of the harmonics as a function of the inverter's load, as per (1):

$$I_{H_n}^{rel} = \frac{I_{H_n}^{abs}}{I_{H_1}^{abs}} \quad (1)$$

where I_{Hn}^{rel} is the relative current for the *n* harmonic [%], I_{Hn}^{abs} is the absolute value for the *n* harmonic [A], and $I_{H_1}^{abs}$ is the absolute value for the fundamental harmonic [A].

For the second study, in order to establish which of the harmonics of the PV plant are proportionally more sensitive to variable power output levels, the measurements were grouped into 22 classes, based on the nominal AC output current at 40° C for each inverter: 0–1%; 1–5%; 5–10%; 10–15%; 15–20%; 20–25%; 25–30%; 30–35%; 35–40%; 40–45%; 45–50%; 50–55%; 55–60%; 60–65%; 65–70%; 70–75%; 75–80%; 80–85%; 85–90%; 90–95%; 95–99% and >99%. Meanwhile, for the substations, the nominal AC output current was calculated by multiplying the nominal AC output current of the inverters connected to each substation by the number of inverters connected, these being 14 type A inverters in substation A, and 20 type B inverters in substation B. Then, for each harmonic (from 2^{nd} up to 50^{th}), the mean value of the measurements belonging to each of the 22 classes was calculated and divided by the maximum value of the corresponding harmonic.

The third study correlates the influence of the current harmonics on the voltage harmonics (from 1^{st} up to 50^{th}), and vice-versa. To this end, a correlation matrix was calculated, using (2).

$$\rho_{xy} = \frac{Cov(x,y)}{\sigma_x \sigma_y} \quad (2)$$

where ρ_{xy} is the Pearson product-moment correlation coefficient, $Cov(x,y)$ is the covariance of variables x and y, σ_x is the standard deviation of x, and σ_y is the standard deviation of y.

Thus, in the correlation matrix, positive values represent a direct relation, in which Y-axis values increase when X-axis values does, and vice versa, whereas negative values represent an inverse relation, in which Y-axis values decrease when X-axis values does, and vice versa. Null values indicate no dependence between the values under study.

IV. Results

The results of the above-mentioned studies are presented in this section, providing an in depth characterization of the current and voltage harmonic emissions of a large utility-scale solar PV power plant in operation.

A. Relative current harmonics distribution

In this section, we calculate the distributions of the relative values of the current harmonics emitted by the two inverters studied and the corresponding substations to which they are connected. In this way, the measured values are delimited, establishing the emission ranges, and characterizing the harmonic pollution in the low voltage network of the photovoltaic installation. The goal is to compare the harmonic emission of the two inverters under similar conditions, which can be performed since both inverters are in the same grid and are located at the same distance (as explained in Section II).

The distributions obtained are shown together by means of a violin plot indicating, vertically, the values of the relative harmonic and, horizontally, the probability of occurrence of those values. Transparency was also used in the proposed plots to highlight the shape of the overlapping distributions. Blue is for inverter and substation A and red is for inverter and substation B. The distributions of harmonics 2 to 15 are also zoomed in for greater detail of these values.

Figure 2(a) shows that, in the harmonic emission spectrum of the inverters, the odd harmonics that are not multiples of 3 stand out. The even harmonics have values lower than 1%, in all cases, except for the outliers in harmonics 2, 4, 6, 8, 10 and 12.

For inverter A, harmonics 5 and 7 are those with the highest values, with a median value of around 1% and maximum values above 10%. The values of harmonic 11, on the other hand, reach values above 6%.

On the other hand, in inverter B, the values of harmonics 5, 7 and 11 are considerably lower in both median and maximum value, not exceeding 5% in any of the cases. However, the ranges of harmonics 13, 19, and odd harmonics greater than 30 and not multiples of 3 are wider.

In the case of the substations, in figure 2(b), the harmonic pattern is very similar. However, in general, an attenuation of the maximum and average values is observed, especially at high frequencies (harmonics 26 and higher). Meanwhile, in the case of substation A, it should be noted that in the range of harmonics 23-25 there is no attenuation and harmonic 24 is considerably increased. Harmonic 17 is attenuated to a greater degree in the case of substation A.

B. Relative current harmonics as a function of the power of the inverter

The aim of this study was to present the relationship between the values of each harmonic and the range of power generated by the inverter or in the substation. For this purpose, the average values of each of the relative harmonics with respect to H1 in bins of power generated each 5% were calculated. Accordingly, a function is obtained that indicates the average value of the harmonics according to the generated power with a resolution of 5% of the total power.

For the representation of the results, a heat map was selected such that all values can be displayed and compared in the same figure. The x-axis of the heat map shows the percentage of power over the maximum power of the corresponding string inverter. The y-axis shows the harmonic analyzed and the color indicates the average value of the relative harmonic per unit in the indicated power range. Hence, it is possible to appreciate the evolution of the relative harmonic values according to the power level.

Figure 3(a) shows the heat map for the harmonics of inverter A. In the even harmonics, there is no dependence on the generated power level. On the other hand, in the odd harmonics, there are different patterns associating the relative harmonic values with the power level. Harmonic 3 shows an increasing trend with power, with a slight drop of around

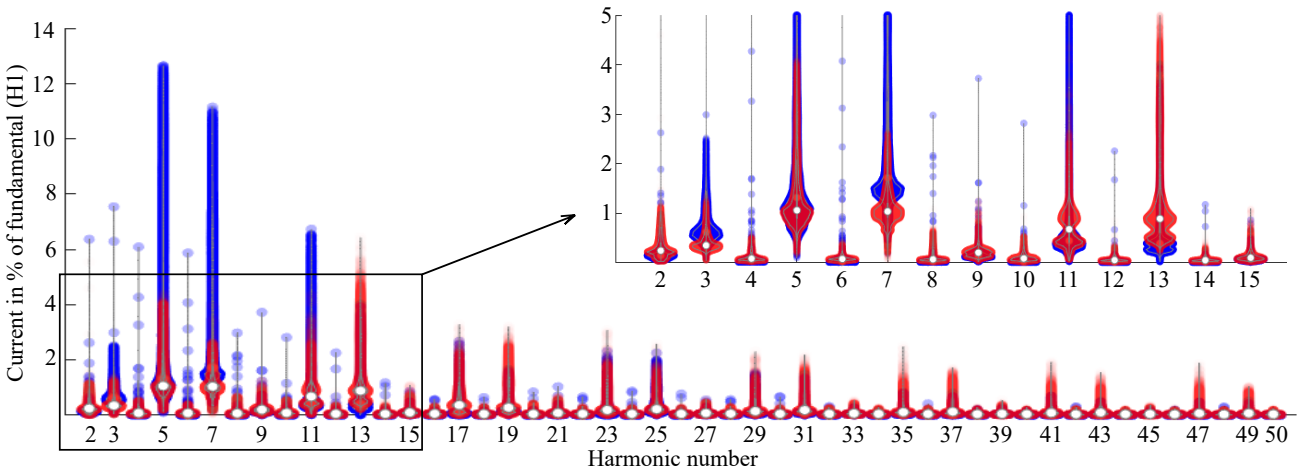

(a) Inverters

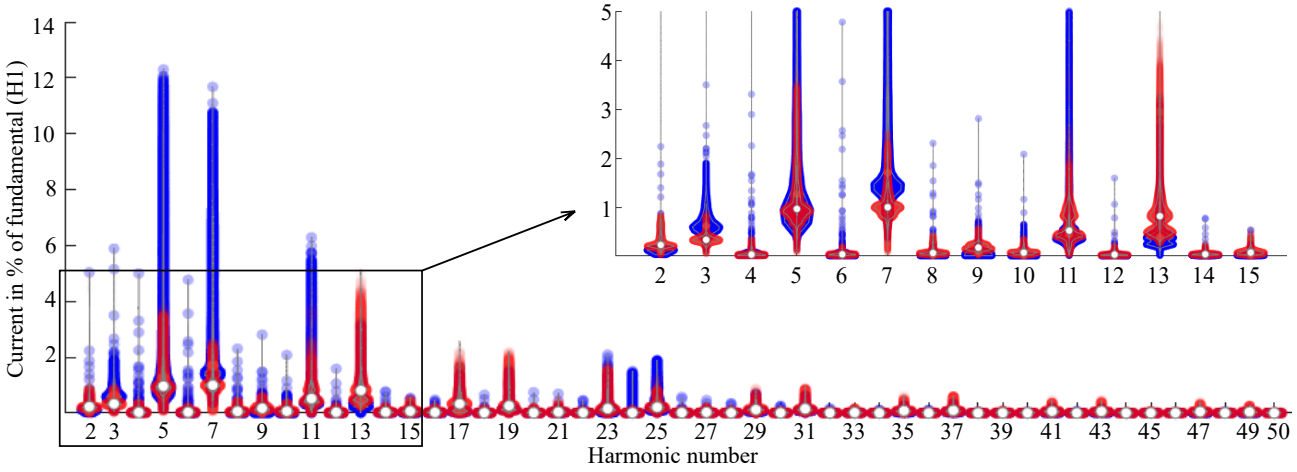

(b) Substations

Fig. 2: Current harmonics relative to H1.

80-85%. Harmonic 5 shows the highest relative values in the power range between 5 and 20 %, with a progressive reduction up to 85 % and finally a further increase up to the maximum generation value. Harmonic 7 shows a maximum of around 35-40%, with a further progressive reduction. The rest of the odd harmonics are represented by two or three relative maxima staggered in different power ranges according to the order of the harmonic.

For inverter B, there is also a stepwise behavior as shown in figure 3(b), but the number of relative maxima is typically 1 and 2. Thus, harmonic 3 presents a constant growth with power, as do harmonics 7 and other multiples of 3 (such as 9, 33, and 39). Harmonics 5, 11 and 13 have the highest values for maximum power, although there are also high values relative to partial powers, 10-15%, 15-20% and 20-25% respectively. Harmonic 19 has the highest relative values in the range 30-40%. The maximum values of the high frequency harmonics are centered at powers above 90%, even in even harmonics such as 24, 26, 28 and 30. Other harmonics, such as 31, 37, 43 and 49, also have a peak relative value at partial load.

Figure 4 shows the results for the substations. In the case of substation A, shown in figure 4(a), the trends of harmonics with power are similar to those obtained for inverter A, although it is worth noting the appearance of notable values at partial loads at high frequency harmonics, such as 25, 29, 31, 37, 43 and 49. In substation B, shown in figure 4(b), the behavior is very similar to that presented by inverter B, but, as in case A, with a greater presence of high frequency harmonics at partial loads.

C. Voltage-current harmonic correlation

The aim of this study was to establish the relationships between voltage and current harmonics measured in the inverters and substations. To establish the relationships, we used the linear or rank correlation coefficient between the relative values of the harmonics for the complete measurement period and in the range from harmonic 1 to 50 for both current and voltage.

To represent the values of the correlation coefficient between the harmonics, a heat map was chosen with the current harmonics on the x-axis, the voltage harmonics on the

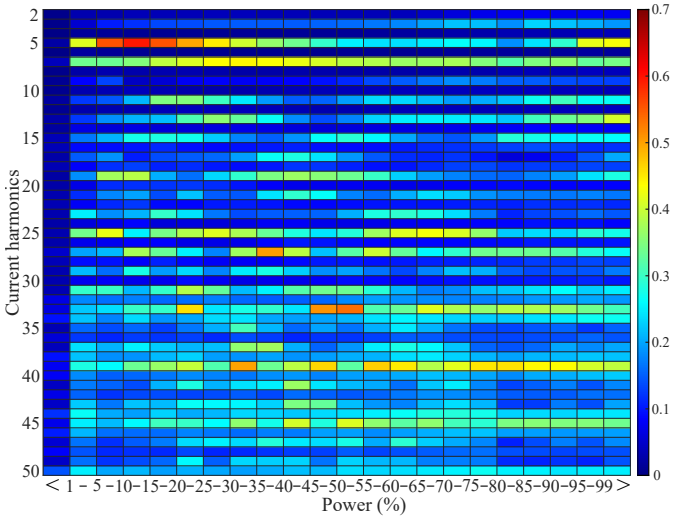

(a) Inverter A

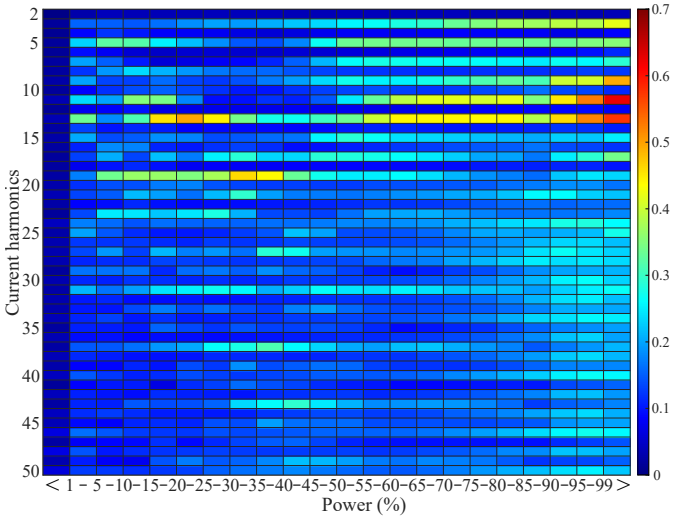

(b) Inverter B

Fig. 3: Harmonic correlation per power loading of the inverters.

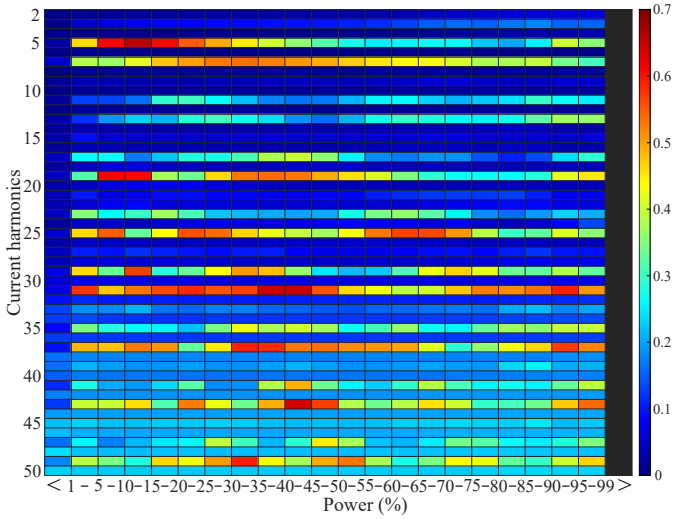

(a) Substation A

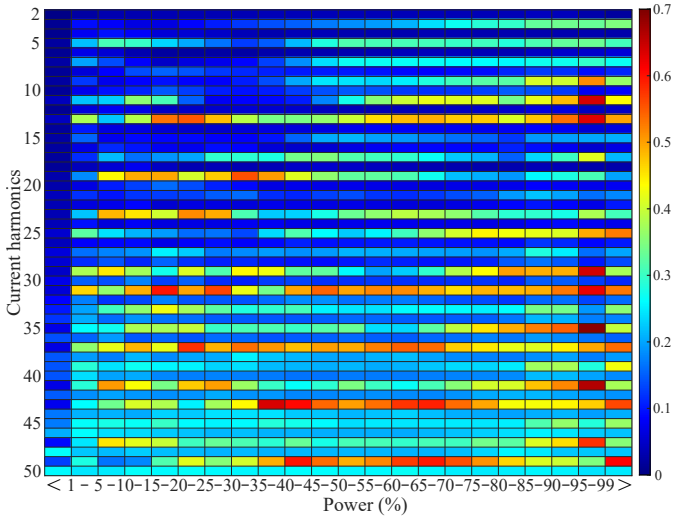

(b) Substation B

Fig. 4: Harmonic correlation per power loading of the substations.

y-axis and the value of the correlation coefficient as a color according to the indicated scale.

Figure 5 shows the heat maps for both inverters. In inverter A, there is a negative correlation between the current harmonics in the range 10-16 and the voltage harmonics. Also noteworthy is a strong correlation between current harmonic 7 and the voltage harmonics. At low frequency, current harmonics 2, 3 and 4 are highly correlated with voltage harmonics 1, 2, 3 and 4. The remaining even harmonics and the fundamental current harmonic have zero or almost zero, correlation with voltage harmonics. At high frequency, the odd harmonics are highly correlated with the whole range of voltage harmonics.

For inverter B, shown in figure 5(b), only negative correlations appear at current harmonics 3 and 12 with the entire range of voltage harmonics. Positive correlations are established between harmonics 2, 8, 9, 10 and the range between harmonics 16 and 50 with all voltage harmonics. As for the null correlation, it is present in the fundamental harmonic 15 and partially in current harmonics 4, 5 and 6.

The results for the substations are shown in figure 6. In the case of substation A, figure 6(a), the positive correlation between current harmonics 2, 3 and 4 and voltage harmonics 1, 2, 3 and 4 is maintained, as well as the negative correlation between current harmonics in the range 10-16 and voltage harmonics. However, a generalized loss of correlation appears in the high frequency currents harmonics, with the entire voltage range, and especially for voltage harmonics above 44.

In substation B, figure 6(b), we obtain very similar results to those for inverter B, with the exception of the appearance of a very high correlation between the harmonics of the same order of current and voltage in the range of 17 to 47. The correlation of voltage harmonics 48 and 50 with the current harmonics also changes considerably.

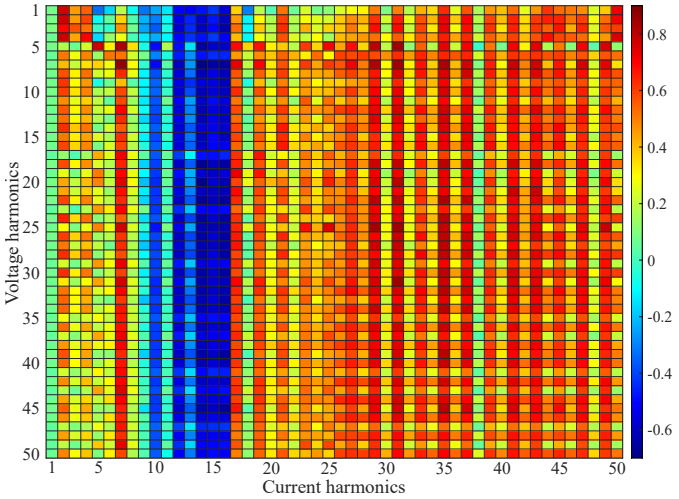

(a) Inverter A

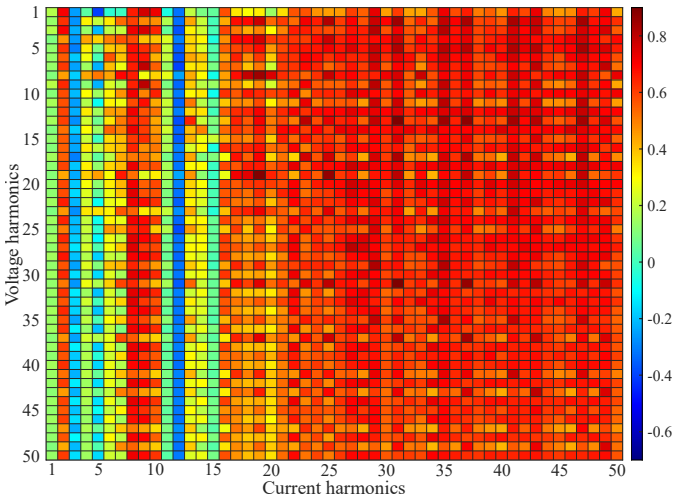

(b) Inverter B

Fig. 5: U-I harmonic correlation of the inverters.

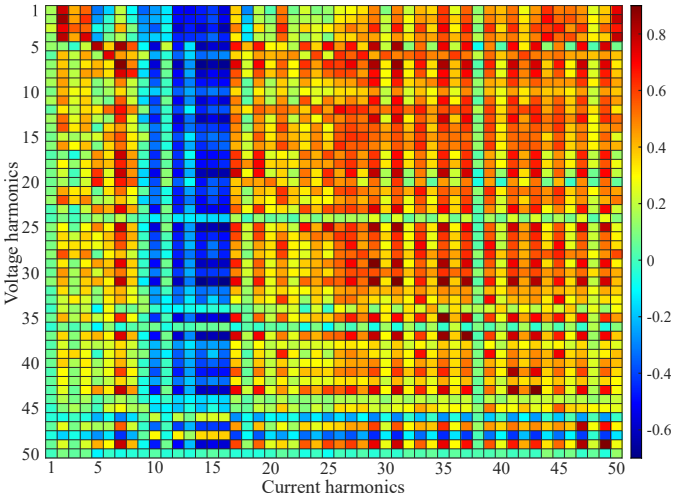

(a) Substation A

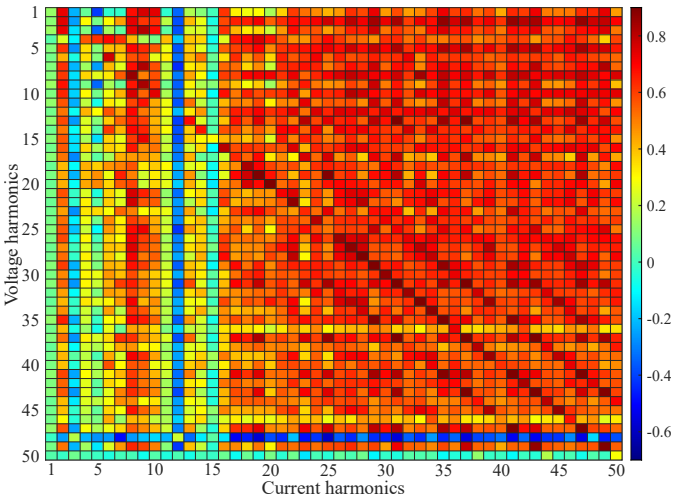

(b) Substation B

Fig. 6: U-I harmonic correlation of the substations.

V. Discussion of the Results

The first study establishes that the main emission by both inverters consists of odd harmonics that are not multiples of 3. However, the prominent harmonics are 5 and 7 for inverter A, and 13 for inverter B. The behavior in the substations is similar to that for the inverters, including a low emission of even harmonics, except in the case of harmonic 24 and a higher attenuation of harmonic 17 in substation A.

The second study shows high heterogeneity in the relationship between power level and harmonic emission. It reveals the existence of relative maxima of most of the harmonics in a staggered way, centered in partial load and full load ranges. The number of maxima is 2-3 for most of the harmonics of inverter A and 1-2 for most of the harmonics of inverter B. In the substations, for both cases, the behavior is very similar to that exhibited by the inverters but with a greater presence of high frequency harmonics at partial loads.

Finally, in the third study, positive, negative and null correlations were identified between current harmonics and voltage harmonics. For the inverter and substation A, positive correlations were identified between groups 2, 3 and 4 for current and 1, 2, 3 and 4 for voltage, current harmonic 7 and the entire range of voltage, and the high frequency odd harmonics with the complete range of voltage harmonics. Null correlations were established between almost all the even harmonics and between the fundamental current harmonic and the entire voltage range. Negative correlations were also shown between current harmonics in the range 10-16 and voltage harmonics. For the inverter and substation B, negative correlations were identified between current harmonics 3 and 12 and the complete range of voltage harmonics. There were positive correlations between harmonics 2, 8, 9, 10 and the range between harmonic 16 and 50 with all the voltage range. There were null correlations between current harmonics 1, 4, 5, 5, 6, and 15 and the complete voltage range.

VI. Conclusions

Studies on the harmonic emissions of PV inverters used in utility-scale power systems are lacking, despite the fact that they account for the majority of the installed solar PV capacity

worldwide. In this regard, the present study is performed in a grid-connected 12 MW PV power plant in operation in Europe.

This paper analyzes the harmonic emissions of two different inverter models in operation, with similar grid conditions, distance to substation and generated power levels, but with different topology and control. The results obtained at inverter level indicate considerable differences in the emitted spectrum, the dependence of harmonics on the generated power level and the correlation between current and voltage harmonics. In the substations, the results obtained were in line to those for the inverters although they shown slight differences due to aggregation.

These findings demonstrate that the emission of current harmonics is greatly influenced by the power loading, as found in the scientific literature. Additionally, under some circumstances, the voltage harmonics and the current harmonics emitted show a strong correlation.

VII. Acknowledgment

This work was supported by the Council of Communities of Castilla–La Mancha (SBPLY/19/180501/000287) and partially supported by the Spanish Ministry of Economy and Competitiveness and the European Union (PID2021-126082OB-C21).

References

[1] "Renewable Energy Statistics 2022," The International Renewable Energy Agency, Tech. Rep., 2022.

[2] "Global Market Outlook For Solar Power 2022 - 2026," Solar Power Europe, Tech. Rep., 2022.

[3] A. Chidurala, T. Saha, and N. Mithulananthan, "Harmonic characterization of grid connected pv systems & validation with field measurements," in 2015 IEEE power & energy society general meeting. IEEE, 2015, pp. 1–5.

[4] J. Sreedevi, N. Ashwin, and M. N. Raju, "A study on grid connected pv system," in 2016 National Power Systems Conference (NPSC). IEEE, 2016, pp. 1–6.

[5] R. Sinvula, K. M. Abo-Al-Ez, and M. T. Kahn, "Total harmonics distortion (thd) with pv system integration in smart grids: Case study," in 2019 International Conference on the Domestic Use of Energy (DUE). IEEE, 2019, pp. 102–108.

[6] A. Chidurala, T. K. Saha, N. Mithulananthan, and R. C. Bansal, "Harmonic emissions in grid connected pv systems: A case study on a large scale rooftop pv site," in 2014 IEEE PES General Meetingl Conference & Exposition. IEEE, 2014, pp. 1–5.

[7] F. Xu, W. Wang, H. Zheng, Z. Luo, K. Guo, and C. Wang, "Harmonic impedance estimation considering the correlation between harmonic sources," Electric Power Systems Research, vol. 209, p. 107947, 2022.

[8] M. Ortega, J. Hernández, and O. García, "Measurement and assessment of power quality characteristics for photovoltaic systems: Harmonics, flicker, unbalance, and slow voltage variations," Electric Power Systems Research, vol. 96, pp. 23–35, 2013.

[9] J. Hernández, M. Ortega, J. De la Cruz, and D. Vera, "Guidelines for the technical assessment of harmonic, flicker and unbalance emission limits for pv-distributed generation," Electric Power Systems Research, vol. 81, no. 7, pp. 1247–1257, 2011.

[10] R. R. Fortes, R. F. Buzo, and L. C. de Oliveira, "Harmonic distortion assessment in power distribution networks considering dc component injection from pv inverters," Electric Power Systems Research, vol. 188, p. 106521, 2020.

[11] S. Sakar, M. E. Balci, S. H. Abdel Aleem, and A. F. Zobaa, "Integration of large- scale pv plants in non-sinusoidal environments: Considerations on hosting capacity and harmonic distortion limits," Renewable and Sustainable Energy Reviews, vol. 82, pp. 176–186, 2018.

[12] F.-J. Ruiz-Rodriguez, J.-C. Hernandez, and F. Jurado, "Harmonic modelling of pv systems for probabilistic harmonic load flow studies," International Journal of Circuit Theory and Applications, vol. 43, no. 11, pp. 1541–1565, 2015.

[13] S. Djokic, J. Meyer, F. Möller, R. Langella, and A. Testa, "Impact of operating conditions on harmonic and interharmonic emission of PV inverters," in 2015 IEEE International Workshop on Applied Measurements for Power Systems (AMPS). IEEE, 2015, pp. 1–6.

[14] X. Xu, A. J. Collin, S. Z. Djokic, R. Langella, A. Testa, J. Meyer, and F. Möller, "Harmonic emission of pv inverters under different voltage supply conditions and operating powers," in 2016 17th International Conference on Harmonics and Quality of Power (ICHQP). IEEE, 2016, pp. 373–378.

[15] R. Langella, A. Testa, J. Meyer, F. Möller, R. Stiegler, and S. Z. Djokic, "Experimental-based evaluation of pv inverter harmonic and interharmonic distortion due to different operating conditions," IEEE Transactions on Instrumentation and Measurement, vol. 65, no. 10, pp. 2221–2233, 2016.

[16] J. C. Hernández, M. J. Ortega, and A. Medina, "Statistical characterisation of harmonic current emission for large photovoltaic plants," International Transactions on Electrical Energy Systems, vol. 24, no. 8, pp. 1134–1150, 2014.